CW-123740-CONF-029
UNRESTRICTED
Revision 0

Code-to-Code Comparisons of Lattice Physics Calculations for Thorium-Augmented and Thorium-Based Fuels in Pressure Tube Heavy Water Reactors

*A. Colton, C. Dugal, B. Bromley and H. Yan
Canadian Nuclear Laboratories – Chalk River
Keys Building, 286 Plant Road, Chalk River, Ontario, Canada K0J 1J0
Phone: 613-584-8811 ext. 43551
*E-mail: ashlea.colton@cnl.ca

ABSTRACT

Code-to-code comparisons of lattice physics calculations were made for a series of fuels that could potentially be used in a conventional 700-MWe class Pressure Tube Heavy Water Reactor to improve the sustainability of the fuel cycle. Studies were performed for natural uranium, slightly enriched uranium and thorium-based fuels containing low enriched uranium, reactor grade plutonium, or $^{233}UO_2$ as the initial fissile driver. The collision probabilities lattice code WIMS-AECL was compared to the stochastic code MCNP using the ENDF/B-VII.0 nuclear data library. Specific parameters that were studied between models include k-infinity, coolant void reactivity, 89-group cell averaged fluence, and ring-by-ring linear element ratings. The calculations performed have demonstrated that physics parameters estimated by WIMS-AECL are consistent with MCNP, especially for fuel where the main fissile component is uranium-based.

Keywords: Lattice physics, Heavy Water Reactors, Code-to-code comparisons, Advanced Fuels, Thorium.

Abbreviations:

PT-HWR: Pressure Tube Heavy Water Reactor

LC: Lattice Concept

CVR: Coolant Void Reactivity

Funding Source:

This research was performed under Canadian Nuclear Laboratories' Federal Science and Technology Energy Program which is paid for through a research contract with the Government of Canada.

Highlights:

- The 2D lattice physics code WIMS-AECL was compared against MCNP using ENDF/B-VII.0.
- Fuels containing mixtures of PuO_2, NUO_2, $LEUO_2$, ThO_2 and $^{233}UO_2$ were modelled.
- 37-element and 35-element bundle geometries for PT-HWR were considered.
- k-inf, LER and CVR agree well for NUO_2, biases appear for (PuO_2/ThO_2),($LEUO_2$/ThO_2).
- 89-group fluxes were calculated and overall show a growing discrepancy with burnup.

1. Introduction

Thorium, a fertile nuclear fuel which is nearly three times as abundant as uranium, represents a long-term energy source that could complement uranium and eventually replace it, leading to sustainable energy production [1]. An initiative is underway at the Canadian Nuclear Laboratories in Chalk River, Ontario to examine and close the gaps that exist between current science and engineering capability and the potential implementation of thorium-based fuels in conventional, operational pressure tube heavy water reactors (PT-HWRs).

A number of fuel types are under investigation as possible short-term and long-term options for incorporating thorium into the fuel cycle of a pressure tube heavy water reactor. The fuel compositions considered range from natural uranium (as a reference case) to mixed oxide fuels composed mostly of thorium dioxide supplemented with a fissile component in the form of either low enriched uranium (5 wt% ^{235}U/U), reactor grade plutonium or ^{233}U. It is expected that the low enriched uranium could be obtained from existing enrichment facilities, the reactor-grade plutonium [2] could be obtained from stockpiles of spent light water reactor fuel and the ^{233}U could be obtained from a future stockpile of spent thorium-based fuels [3].

In a previous study [4], full core physics calculations were performed using the neutron diffusion code RFSP [5] for a number of uranium-based test fuels augmented with thorium in a PT-HWR core. The effects of leakage and online refuelling were modelled in RFSP and key physics parameters such as the full core average burnup, refuelling rates, the maximum bundle and channel powers, and the power distribution were evaluated.

To obtain irradiated fuel compositions, WIMS-AECL [6] is used to perform lattice-level collision probabilities based depletion calculations, which are homogenized into two group macroscopic

cross-sections for the full core RFSP diffusion model. The accuracy of the deterministic core physics calculations with RFSP depends directly on the deterministic lattice physics calculations performed using WIMS-AECL. Therefore, the purpose of this work is to build confidence in lattice physics modelling performed in WIMS-AECL by comparing analogous models built in the continuous energy transport code MCNP [7].

2. Description of Lattice Concepts

The lattice concepts described here were modelled with the average operating parameters of a 380-channel 2061 MW_{th} PT-HWR. The two types of fuel bundle geometries studied in this work were a 37-element bundle and a 35-element bundle, as illustrated schematically in Figures 1a and 1b, respectively.

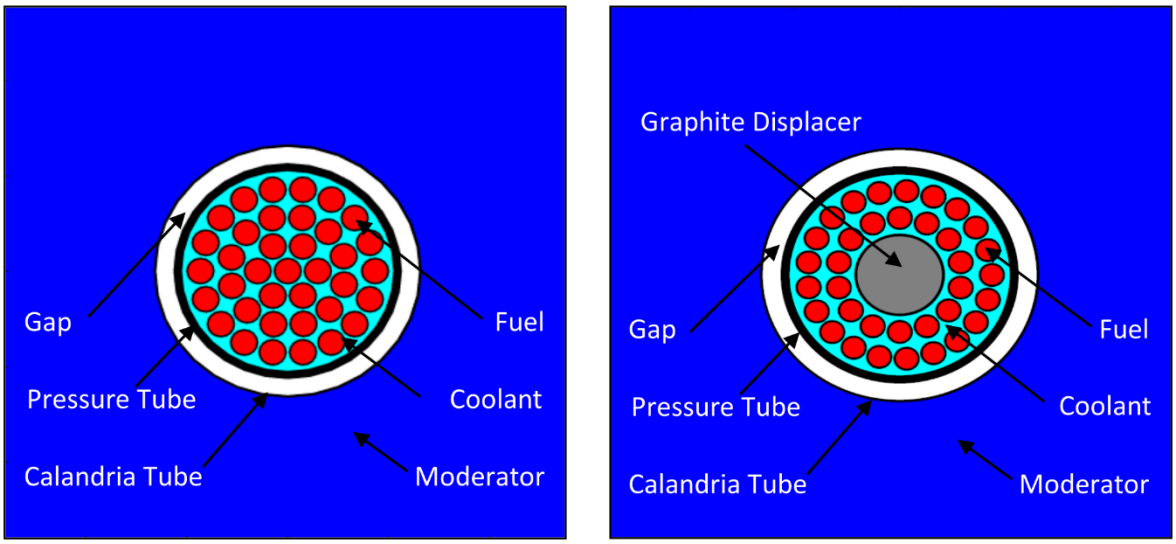

Figure 1a: 37-Element Lattice Cell Geometry (left) and Figure 1b: 35-Element Lattice Cell Geometry (right).

The outermost region of the lattice depicts the heavy water (D_2O) moderator, which is separated from the fuel channel by a Zircaloy-2 calandria tube (Figures 1a and 1b). A CO_2 gas annulus separates the calandria tube from the pressure tube, which is composed of Zr-2.5% Nb. The pressure tube contains

heavy water coolant and the fuel bundle. The fuel bundle assembly consists of Zircaloy-4 fuel elements, welded together in a cluster formation and filled with oxide fuel pellets. The geometric specifications for the fuel channel and fixed components of the lattice are given in Table 1 and the estimated average operating temperatures and materials of the non-fuel components in this lattice are specified in Table 2. The specific geometric data for the 35-element and 37-element bundles are provided in Table 3. The fuel bundle materials, densities, specific powers and estimated average operating temperatures are given in Table 4.

Table 1
Geometric Specifications for the Fuel Channel and Fixed Lattice Components

Geometric Description	Value (cm)
Lattice Pitch	28.6
Pressure Tube Inner Radius	5.17
Pressure Tube Outer Radius	5.60
Calandria Tube Inner Radius	6.45
Calandria Tube Outer Radius	6.59

Table 2
Average Operating Temperatures and Materials of Fuel Channel Components

Structure	Temperature (K)	Material	Density (g/cm^3)
Coolant	561	99.1 wt% D_2O	0.81
Voided Coolant	561	99.1 wt% D_2O	0.001
Pressure Tube	561	Zr-2.5Nb	6.52
Gap	451	CO_2	0.0012
Calandria Tube	342	Zr-2	6.54
Moderator	342	99.75 wt% D_2O	1.09
Central Displacer Rod	561	Nuclear Grade Graphite	1.50

Table 3
Geometric Specifications of the 35-Element and 37-Element Fuel Bundles

Quantity		BUNDLE-37	BUNDLE-35	Units
Bundle Length		49.53	49.53	cm
Fuel Stack Length		48.0	48.0	cm
Total Fuel Elements		37	35	#
Fuel Pellet Outer Radius		0.61	0.53	cm
Fuel Element Outer Radius		0.65	0.57	cm
Central Moderating Element Radius		—	1.95	cm
Central Displacer Rod Cladding Outer Radius		—	2.10	cm
Ring 1	Fuel Elements	1	14	ele/ring
	Pitch Circle Radius	0	2.97	cm
	Angular Offset	0	12.8	degrees
Ring 2	Fuel Elements	6	21	ele/ring
	Pitch Circle Radius	1.49	4.38	cm
	Angular Offset	0	0	degrees
Ring 3	Fuel Elements	12	-	ele/ring
	Pitch Circle Radius	2.87	-	cm
	Angular Offset	15	-	degrees
Ring 4	Fuel Elements	18	-	ele/ring
	Pitch Circle Radius	4.32	-	cm
	Angular Offset	0	-	degrees

Table 4
37-Element and 35-Element Fuel Bundle Materials, Densities, Specific Powers and Estimated Average Operating Temperatures

Quantity	BUNDLE-37	BUNDLE-35	Units
Temperatures			
Fuel	941	941	K
Clad	751	751	K
Materials			
Central Moderating Element	—	Graphite	—
Clad	Zr-4	Zr-4	—
Densities			
Zr-4 Fuel Cladding	6.46	6.46	g/cm^3
Graphite Centre Element	—	1.5	g/cm^3
Uranium-based Fuel	10	10	g/cm^3
Plutonium-based Fuel	—	9.7	g/cm^3
Thorium-based Fuel	9.7	9.7	g/cm^3
Power			
Specific Power in Seed Fuel	31.5	46.0	W/gHE
Specific Power in Blanket Fuel	8.5	11.49	W/gHE

Six types of fuel were compared in this work; these fuels were mixed with thorium dioxide in different ratios to achieve specific target burnup values. The weight percent composition of each fuel type studied is given in Table 5. The fuel types examined are all in oxide form and include natural uranium (NU), recovered uranium (RU) at 0.95 wt% $^{235}U/U$, slightly enriched uranium (SEU) at 1.2 wt% $^{235}U/U$, low enriched uranium (LEU) at 5 wt% $^{235}U/U$, reactor grade plutonium, and pure ^{233}U.

Table 5
Fuel Compositions and densities in weight percent

Fuel Type	Nuclide	Nuclide Amounts (wt%)	Nominal Density (g/cm^3)
Natural UO_2	U234	4.68E-03	10.0
	U235	6.27E-01	
	U238	8.75E+01	
	O16	1.18E+01	
	O17	4.79E-03	
RU (0.95 wt% U-235/U)	U234	4.67E-03	10.0
	U235	8.37E-01	
	U238	8.73E+01	
	O16	1.18E+01	
	O17	4.78E-03	
SEU (1.2 wt% U-235/U)	U234	4.66E-03	10.0
	U235	1.06E+00	
	U238	8.71E+01	
	O16	1.18E+01	
	O17	4.78E-03	
LEU (5 wt% U-235/U)	U234	3.37E-02	10.0
	U235	4.42E+00	
	U238	8.40E+01	
	O16	1.19E+01	
	O17	4.81E-03	
ThO_2	TH232	8.79E+01	9.7
	O16	1.21E+01	
	O17	4.89E-03	
PuO_2	PU238	2.43E+00	9.7
	PU239	4.58E+01	
	PU240	2.03E+01	
	PU241	1.34E+01	
	PU242	6.26E+00	
	O16	1.18E+01	
	O17	4.75E-03	
$^{233}UO_2$	U233	8.87E+01	10.0
	O16	1.13E+01	
	O17	4.92E-03	

Small amounts of thorium (1-2% by volume) were added to the fuel with the intent of grading the fissile content of the fuel stack horizontally to mitigate end power peaking [8].

In this study we modelled a series of lattice concepts as described in Table 6. The table provides a number of details used to model each concept including the central element material, the outer ring material, the relative power of the bundle, and the total amount of thorium mixed into the end pellets of the fuel specified in length of end pellets.

Table 6
Lattice Concept Description

Lattice Concept	Relative Power (W/gHE)	Bundle Geometry	Materials of Central Element	Materials of Outer Fuel Rings	Total End Pellet Length (cm)*
LC-01	31.5	37-element	100 wt% NUO_2	100 wt% NUO_2	—
LC-02	31.5	37-element	100 wt% NUO_2	100 wt% NUO_2	1
LC-03	8.5	37-element	100 wt% ThO_2	100 wt% ThO_2	—
LC-04b	31.5	37-element	100 wt% ThO_2	100 wt% RUO_2	2
LC-05b	31.5	37-element	100 wt% ThO_2	100 wt% $SEUO_2$	2
LC-06b	45.96	35-element	100 wt% Graphite	3.5 wt% PuO_2 + 96.5 wt% ThO_2	2
LC-08b	45.96	35-element	100 wt% Graphite	4.5 wt% PuO_2 + 95.5 wt% ThO2	2
LC-10b	45.96	35-element	100 wt% Graphite	40 wt% $LEUO_2$ + 60 wt% ThO_2	2
LC-12b	45.96	35-element	100 wt% Graphite	50 wt% $LEUO_2$ +50 wt% ThO_2	2
LC-14b	45.96	35-element	100 wt% Graphite	1.8 wt% $^{233}UO_2$ + 98.2 wt% ThO_2	2
LC-16b	11.49	35-element	100 wt% Graphite	100 wt% ThO_2	—

* In reality, pure ThO_2 end pellets would not be used. The amount of ThO_2 specified in the "end pellets" would be mixed with the same type of fuel used in the main fuel stack. ThO_2 would be used to down-blend the fuel to a lower fissile content, and would be used in the last 2-3 cm of fuel at either end of the fuel stack.

The 37-element natural uranium fuel bundle (Figure 1a), with four fuel rings of fuel elements in a cluster geometry, is the standard fuel design used in many operating PT-HWRs. The 35-element bundle [9] consists of a central enlarged displacer rod and two outer rings of fuel elements. This bundle is intended for advanced mixed oxide fuel types and is developed to reduce coolant void reactivity by removing the inner fuel rings. Some lattice concepts (LC-07b, LC-11b, LC-13b, LC-15b) are omitted from the table as

they belong to fuel bundle configurations that are being assessed at Canadian Nuclear Laboratories, but are not discussed in this work.

3. Analysis Methodology

3.1 WIMS-AECL Lattice Physics Analysis:

The lattice physics code WIMS-AECL version 3 [6] is used for depletion calculations. It is a deterministic code that solves the integral form of the neutron transport equation in a fixed number of energy groups using the collision probabilities method. An 89 energy group nuclear data library [10] based on ENDF/B-VII.0 was used with WIMS-AECL.

WIMS-AECL lattice depletion models were prepared for each case described in Table 6. The component temperatures, geometries and densities used are shown in Tables 1 – 4 and the fuel compositions given in Table 5 were then used to create the specific fuel mixtures described in Table 6. A depletion calculation was carried out to establish an estimate of the exit burnup of the fuel. The depletion time steps (Table 7) were varied, with smaller initial time steps to capture steep lattice reactivity changes at low burnup, followed by larger time steps as the variance in k-infinity decreases with higher burnup.

Table 7
WIMS-AECL Depletion Time Steps

Step Length (d)	Steps Taken
0.1	1
0.2	1
0.3	2
0.4	1
0.6	1
0.7	1
1.0	1
1.3	1
1.6	1
2.0	22
2.5	20
2.5	196
5.0	146

The parameters compared here for each fuel type were extracted at three burnup steps: fresh, mid-burnup and exit burnup. The full core exit burnup for each fuel type was estimated from an infinite lattice depletion calculation when the burnup-averaged k-infinity was equal to 1.050. The excess 0.05 k was allocated to account for reactivity control devices used during reactor operation and for neutron leakage. For each depletion case, a fixed relative power in watts/gram-heavy-element (W/gHE) was used based on the case list given in Table 6, corresponding to an approximate bundle power of 600 kW for seed or fissile fuel and 150 kW for pure thorium blanket fertile fuel. The depletion calculation was performed using a critical spectrum where WIMS-AECL adjusted the imposed buckling until the lattice achieved a k-effective value of 1.000. The fuel compositions at each burnup step were output to a file for later use. These compositions were then read in by WIMS-AECL to perform a perturbation study by changing the coolant density to 0.001 g/cm^3 to simulate a voided condition.

Certain aspects of the fuel could not be captured by modelling the bundle in two dimensions. For example, the fuel bundle end plates and end caps were not modelled explicitly. Instead, the representative quantity of Zr-4 was smeared throughout the fuel sheath by scaling up its density by a factor of 1.13 in both codes. The axially heterogeneous fuel segments, namely the thorium pellets in the end regions were smeared homogeneously into the main fuel stack since they could not be modelled explicitly in a 2D model.

3.2 MCNP Lattice Physics Analysis:

MCNP 5 v 1.40 is a stochastic, general purpose, continuous energy, monte-carlo based n-particle transport code [7]. It can be used to model the transport of neutrons, gamma rays, and electrons. A continuous energy nuclear data library based on ENDF/B-VII.0 was used with MCNP for this work [10].

The resultant fuel compositions for fresh, mid-burnup and exit-burnup fuels were taken from the WIMS-AECL analysis and used in three static MCNP calculations. Corresponding models were also prepared using the same fuel compositions but with a voided coolant state for the purpose of comparing the coolant void reactivity (CVR). The CVR was evaluated as:

$$CVR = 1000\left(\frac{1}{k_{cool}} - \frac{1}{k_{void}}\right) \text{(mk)} \quad (1)$$

where k_{cool} is k-infinity for the cooled lattice cell and k_{void} is k-infinity for the voided lattice cell. The geometries and temperatures in the MCNP model matched the WIMS-AECL model exactly. The MCNP model was made with reflective boundary conditions. A kcode type calculation was performed to find the k-infinity value using 100,000 neutrons per cycle with 20 inactive cycles followed by 100 active cycles translating into a k-effective statistical uncertainty of ±0.2 mk or less.

The subsequent statistical uncertainty in the CVR calculation was calculated by:

$$\sigma_{CVR}^2 = \frac{{\sigma_{cool}}^2}{{k_{cool}}^4} + \frac{{\sigma_{void}}^2}{{k_{void}}^4} \quad (2)$$

where k_{cool} and k_{void} are the k-infinity values for the cooled and voided MCNP cases and the σ_{cool} and σ_{void} are their corresponding statistical uncertainties.

The MCNP model contains F4 type tallies that track the 89-group neutron energy spectra homogenized over the lattice cell. Results from the MCNP tallies required scaling to estimate the total recoverable power such that the relative power density was analogous to the calculation done by WIMS-AECL. The total prompt energy release per source neutron was calculated for all of the fuels using an F7 tally. This total prompt energy was scaled by a factor of 1.07 to account for delayed gamma and delayed beta radiation. The constant scaling factor is an approximation, as it varies across fissile nuclides by less than 2%. The target bundle power was divided by the total recoverable fission energy per source neutron to arrive at the neutron source strength. All tally results were scaled by the neutron source strength.

4. Results

6.1 Natural Uranium 37-Element Fuel Bundle Literature Review and Result Comparison

Given that the 37-element natural uranium bundle has been studied extensively, it is considered prudent to compare the current results using LC-01 (NU fuel) with those in previous studies [11, 12, 13] to ensure that the results are consistent. The works of Nuttin et al. [11, 12] considered a 450 kW 37-element NU bundle modelled using both DRAGON and MCNP coupled with MURE for depletion calculations. Nuclear data libraries based on ENDF/B-VI with the IAEA 172 group structure were

employed for deterministic calculations. Some small differences in material temperatures exist between analyses.

Results from Nuttin et al. are summarized in Table 8, the predicted fresh fuel CVR values between DRAGON [9] and WIMS-AECL for LC-01 agree well, as do the MCNP CVR values. The exit burnup predicted by DRAGON is within 0.3% of discharge burnup found for LC-01. The fresh fuel DRAGON calculated k-infinity was obtained from the same analysis and is found to be 9.2 mk lower than the fresh k-infinity obtained from WIMS-AECL for LC-01, which is expected based on past analysis comparing ENDF/B-VI to ENDF/B-VII [8].

Table 8
Code to Code Comparison from Literature for Natural Uranium, 37-Element Infinite Lattice Physics Studies

Parameter	A. Nuttin 2006	A. Nuttin 2011	G. Roh 2000	A. Colton	
Bundle Power	450 kW	450 kW	-	600 kW	
Deterministic Code	DRAGON	DRAGON	WIMS-AECL	WIMS-AECL	
Library	IAEA ENDF/B-VI	IAEA ENDF/B-VI	ENDF/B-VI	ENDF/B-VII	
Energy Groups	172	172	89	89	-
Fresh k-infinity cooled	-	1.1119	-	1.1211	-
Fresh CVR	15.5	-	16.9	16.1	mk
Exit CVR	11.8	-	14.1	13.5	mk
Predicted Exit Burnup	7273	-	7228	7261	MWd/THE
Stochastic Code	MCNP + MURE	MCNP	MCNP-4	MCNP 5	
Fresh k-infinity cooled	-	1.1164	-	1.1142	-
Fresh CVR	16.9	-	16.3	16.7	mk
Exit CVR	12.7	-	13.9	13.8	mk

Similar calculations were performed by Roh et al. [13] while benchmarking different nuclear data libraries (Table 8). Their work consisted of using the deterministic code WIMS-AECL for infinite lattice calculations of natural uranium, 37-element fuel bundles in 89 groups and then preparing analogous models in MCNP-4 with libraries based on ENDF/B-VI. The deterministic CVR values between WIMS-

AECL results agree well with those calculated for LC-01, as do the MCNP predicted values. Additionally, the Roh study contained the relative pin powers for fresh fuel, which are duplicated and compared alongside present results in Table 9. The ring-by-ring pin powers across codes from Roh and LC-01 match to within 0.3%. Based on the above comparisons, the MCNP and WIMS-AECL models prepared for LC-01 agree with the available literature for the parameters that were compared.

Table 9
Relative Pin Power Comparison from Literature for Fresh Natural Uranium, 37-Element Infinite Lattice Calculation

	G. Roh, 2000	A. Colton	
	WIMS-AECL	WIMS-AECL	Delta
Ring 1	0.214	0.213	0.001
Ring 2	0.223	0.224	-0.001
Ring 3	0.252	0.251	0.001
Ring 4	0.313	0.312	0.001
	MCNP	MCNP	Delta
Ring 1	0.211	0.211	0.000
Ring 2	0.222	0.222	0.000
Ring 3	0.252	0.253	-0.001
Ring 4	0.315	0.314	0.001

6.2 37-Element Bundle Results

The k-infinity and CVR results for the 37-element lattice calculations from both WIMS-AECL and MCNP are shown in Table 10 alongside the MCNP statistical uncertainties. For uranium-based 37-element fuel types, the average k-infinity bias is +0.3 mk, quite close to the MCNP uncertainty. The average CVR bias is even smaller at -0.1 mk. The CVR and subsequent bias for the fresh thorium bundle (LC-03) is high due to the highly sub-critical nature of pure thorium fuel (k-infinity ~ 0.04) which causes the overall CVR uncertainty in the MCNP calculation to rise. With a small k-infinity value, the statistical uncertainty in MCNP can result in significant differences in CVR. The code-to-code k-infinity bias for mixed uranium

and thorium fuels (LC-02/LC-04b/LC-05b) exhibits a trend where the fresh fuel bias is the largest and it decreases with the depletion of the fuel.

Table 10
37-Element Lattice Concept Results for MCNP5/WIMS-AECL $k_{inf-cool}$, $k_{inf-void}$ and CVR

Burnup	MCNP						WIMS-AECL			WIMS-AECL - MCNP		
	k_{cool}	σ_{cool}	k_{void}	σ_{void}	CVR	σ_{CVR}	k_{cool}	k_{void}	CVR	Δk_{cool}	Δk_{void}	ΔCVR
MWd/THE	-	-	-	-	mk	mk	-	-	mk	mk	mk	mk
LC-01 NUO_2 Fuel												
3.2	1.1142	0.00013	1.1353	0.00012	16.7	0.14	1.1144	1.1349	16.1	0.2	-0.5	-0.6
3,641.00	1.0548	0.00014	1.0700	0.00016	13.5	0.19	1.0538	1.0690	13.5	-1.0	-1.0	0.0
7,261.50	0.9931	0.00015	1.0070	0.00014	13.8	0.21	0.9922	1.0057	13.5	-1.0	-1.3	-0.3
LC-02 **N**UO_2 Fuel												
3.2	1.0875	0.00013	1.1084	0.00013	17.3	0.15	1.0886	1.1089	16.8	1.1	0.6	-0.5
2,223.50	1.0538	0.00013	1.0696	0.00013	14	0.16	1.0537	1.0696	14.1	-0.1	0	0.1
4,428.80	1.0258	0.00013	1.0404	0.00012	13.7	0.17	1.0255	1.0403	13.8	-0.2	-0.1	0.1
LC-03 ThO_2 Fuel												
0.4	0.0355	0.00001	0.0370	0.00001	1130.6	10.76	0.0359	0.0374	1163.5	0.3	0.4	32.9
2,501.40	0.7962	0.00011	0.8052	0.00009	13.9	0.22	0.7967	0.8054	13.6	0.6	0.3	-0.4
5,010.60	0.8696	0.00011	0.8793	0.00011	12.7	0.20	0.8703	0.8782	10.3	0.6	-1.2	-2.4
LC-04b RUO_2 Fuel												
3.2	1.1643	0.00013	1.1835	0.00013	13.9	0.13	1.1656	1.1846	13.8	1.4	1.2	-0.2
5,527.50	1.0520	0.00014	1.0668	0.00013	13.2	0.17	1.0526	1.0676	13.3	0.6	0.8	0.1
11,036.20	0.9655	0.00016	0.9793	0.00013	14.6	0.22	0.9661	0.9795	14.1	0.6	0.2	-0.5
LC-05b $SEUO_2$ Fuel												
3.2	1.2563	0.00014	1.2761	0.00013	12.3	0.12	1.2579	1.2774	12.1	1.6	1.3	-0.2
9,144.00	1.0510	0.00015	1.0663	0.00015	13.7	0.19	1.0515	1.0673	14.0	0.6	0.9	0.3
18,428.30	0.9151	0.00016	0.9273	0.00014	14.4	0.25	0.9153	0.9278	14.8	0.2	0.5	0.4

The linear element ratings (LER) for the cooled 37-element bundle geometry are given in Table 12. The WIMS-AECL and MCNP predictions are within 1% in the outermost two rings of fuel and are within 4% in the inner two rings of fuel. The larger LER differences occur in the centre of the fuel bundle in all cases. The central element LER predictions improve in agreement for the thorium central element cases as

fissile material is bred in; at discharge burnup the code percent differences are reduced to at most 2%. Overall, the agreement between codes is good for the radial power distribution in the bundle.

Table 11
BUNDLE-37 MCNP5/WIMS-AECL Cooled Linear Element Ratings

Burnup (MWd/THE)	MCNP5 LER (kW/m)				WIMS-AECL LER (kW/m)				% Difference			
	Ring 1	Ring 2	Ring 3	Ring 4	Ring 1	Ring 2	Ring 3	Ring 4	Ring 1	Ring 2	Ring 3	Ring 4
LC-01 UO_2												
3.2	24.8	26.1	29.7	36.9	25.2	26.4	29.7	36.8	1.5%	1.0%	0.2%	-0.4%
3641.0	24.9	26.2	29.7	36.8	25.3	26.5	29.8	36.7	1.7%	1.1%	0.2%	-0.4%
7261.5	25.5	26.8	30.0	36.5	26.0	27.1	30.0	36.3	1.9%	1.0%	0.2%	-0.4%
LC-02 UO_2												
3.2	24.8	26.1	29.7	36.9	25.2	26.4	29.7	36.8	1.7%	1.0%	0.2%	-0.4%
2223.5	24.6	26.0	29.6	37.0	25.0	26.3	29.7	36.9	1.8%	1.1%	0.2%	-0.4%
4428.8	25.0	26.3	29.8	36.8	25.4	26.6	29.8	36.7	1.7%	1.1%	0.2%	-0.4%
LC-03 ThO_2												
0.4	7.8	7.9	8.4	9.3	7.7	7.8	8.2	9.0	1.6%	1.4%	0.6%	-0.8%
2501.4	4.8	5.3	7.0	11.3	4.8	5.3	6.8	10.9	2.7%	1.8%	0.6%	-0.6%
5010.6	4.8	5.4	7.0	11.3	4.8	5.3	6.9	10.8	3.0%	1.9%	0.6%	-0.6%
LC-04b RUO_2												
3.2	0.3	25.7	29.8	38.3	0.3	26.0	29.9	38.2	2.9%	1.3%	0.3%	-0.4%
5527.5	11.2	26.4	30.0	37.4	11.4	26.7	30.1	37.2	1.2%	1.2%	0.3%	-0.4%
11036.2	21.8	26.9	30.0	36.6	22.1	27.2	30.1	36.4	1.4%	1.2%	0.3%	-0.5%
LC-05b $SEUO_2$												
3.2	0.3	24.9	29.3	38.9	0.3	25.2	29.4	38.8	4.2%	1.3%	0.3%	-0.4%
9144.0	14.2	26.8	30.3	36.9	14.4	27.2	30.3	36.7	1.5%	1.2%	0.2%	-0.4%
18428.3	27.7	27.1	29.9	36.3	28.1	27.4	30.0	36.1	1.6%	1.3%	0.2%	-0.5%

The 89-group cell averaged neutron flux per unit lethargy was calculated for each fuel type studied in the 37-element fuel bundle geometry and is shown in Figure 3. The percent differences with WIMS-AECL for the 89-group fluxes are shown in Figure 4. The LC-02 results are similar to LC-01 and are therefore omitted from the summary plots. The magnitude of the flux for LC-03 is larger for fresh fuel as it contains no fissile material, only Th-232, and therefore relies on fast fissions to produce a power of

150 kW. Clearly LC-03 has larger discrepancies in the thermal range than any other fuel. In addition, the other fuel types show similar behavior in terms of the percent difference shape, but with a varying bias.

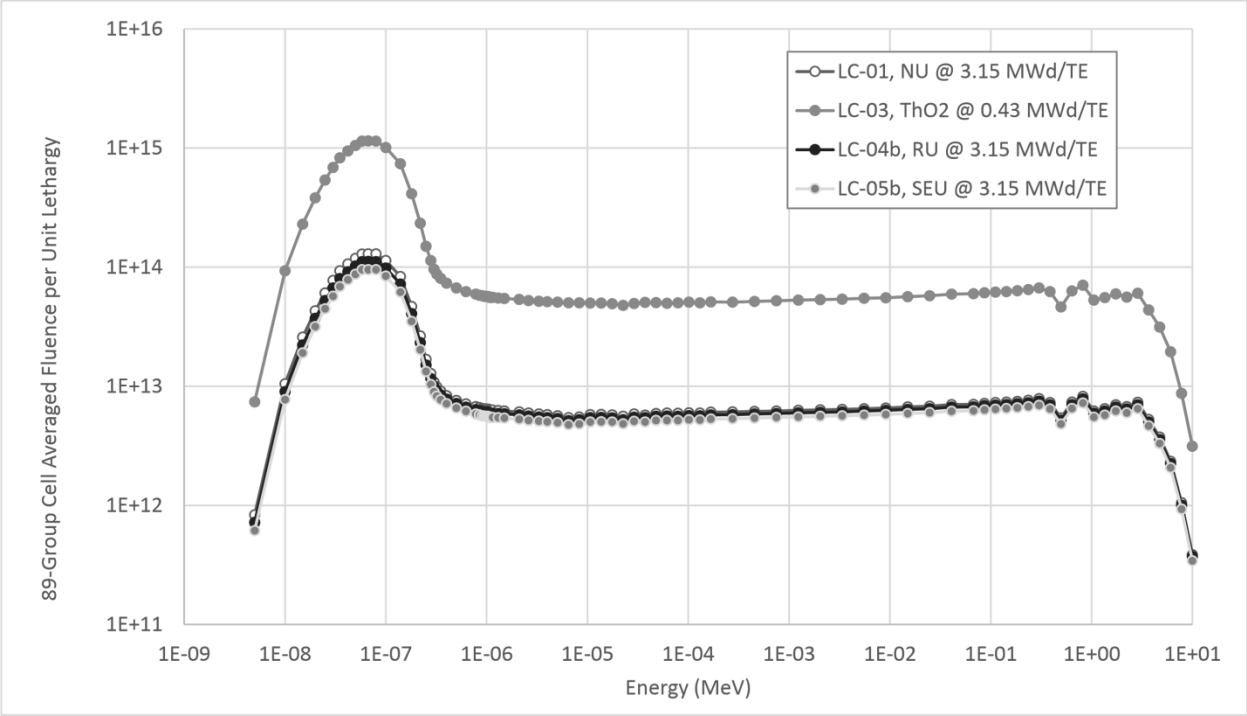

Figure 3: 89 Group Lethargy Normed MCNP Calculated Neutron Flux for 37-Element Fuel Bundle in Cooled State WIMS-AECL and MCNP (bottom) for 37-Element, Fresh Fuels in Cooled State.

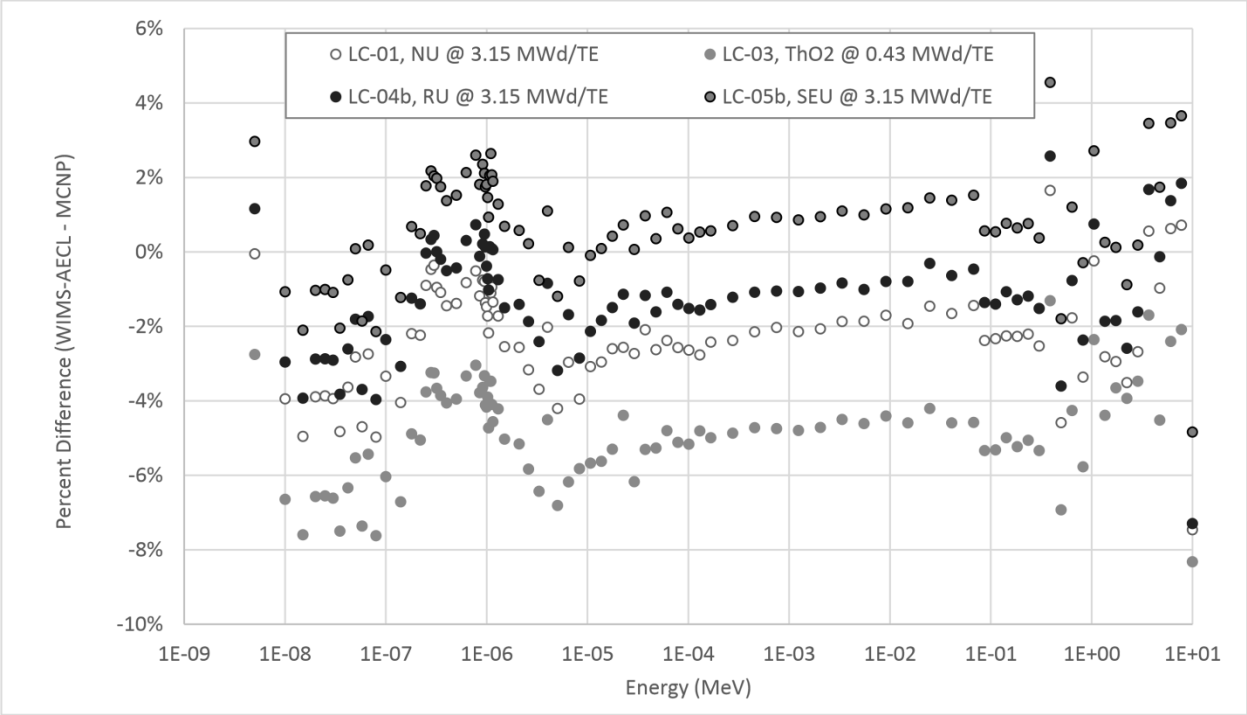

Figure 4: 89 Group Lethargy Normed MCNP Calculated Neutron Flux Percent Difference between WIMS-AECL and MCNP for 37-Element, Fresh Fuels in Cooled State.

The relative error was evaluated to determine the level of agreement between WIMS-AECL and MCNP 89-group cell-averaged flux values. Relative error was calculated as:

$$Error = \frac{\sum_{g=1}^{G} \left| \Phi_{WIMS,g} - \Phi_{MCNP,g} \right|}{\sum_{g=1}^{G} \Phi_{MCNP,g}} \cdot 100\% \quad (3)$$

where the term $\Phi_{WIMS,g}$ is the cell-averaged flux calculated by WIMS-AECL at energy bin 'g', similarly $\Phi_{MCNP,g}$ is the cell-averaged flux calculated by MCNP at energy bin 'g'. The relative error for all 37-element cell-averaged 89-group flux calculations are provided in Table 13 and show that overall, the discrepancies between WIMS-AECL and MCNP increase with burnup for both cooled and voided calculations (with the exception of the pure thorium bundle). The pure thorium bundle represents an

interesting case, as the k-infinity values calculated between WIMS-AECL and MCNP were quite close (~0.6 mk), however this relative error metric shows that there are greater discrepancies which may be cancelling out (5-6%).

Table 12
89-Group Cell Averaged Lethargy Normed Flux Relative Error Estimates for 37-Element Fuel

Case	Fuel Type	Burnup (MWd/THE)	Cool Error (%)	Void Error (%)
LC-01		3.15	3.3	2.7
LC-01	NUO_2	3641.01	4.0	3.7
LC-01		7261.47	5.0	4.8
LC-02		3.15	3.7	3.2
LC-02	NUO_2	2223.53	4.0	3.7
LC-02		4428.75	4.5	4.2
LC-03		0.43	5.9	6.0
LC-03	ThO_2	2501.41	4.4	4.4
LC-03		5010.64	4.5	4.4
LC-04b		3.15	2.3	1.8
LC-04b	RUO_2	5527.53	4.0	3.7
LC-04b		11036.21	5.5	5.2
LC-05b		3.15	1.1	1.1
LC-05b	$SEUO_2$	9144.03	4.0	3.7
LC-05b		18428.34	6.4	6.3

6.3 35-Element Bundle Results

The 35-element lattice calculations of k-infinity and CVR are provided in Table 14. For the plutonium-based fuels, the average cooled k-infinity bias between WIMS-AECL and MCNP is -4.8 mk, where higher k-infinity values are predicted by MCNP. The implications of this result (assuming that MCNP is closer to reality) may be that WIMS-AECL is underestimating the exit burnup. A bias of +4 mk (where MCNP predicts lower k-infinity values) is observed for LEU/thorium fuels. The ^{233}U/thorium fuels exhibit a +1.2 mk average bias for cooled k-infinity, which drops to +0.4 mk for the voided cases. Pure

thorium fuel exhibits better agreement than the other studied cases with a +0.6 mk average bias for cooled k-infinity, which is comparable to the bias in LC-03.

Table 13
BUNDLE-35 MCNP5/WIMS-AECL k_{eff}, k_{eff_void} and CVR

Burnup	MCNP						WIMS-AECL			WIMS-AECL - MCNP		
	k_{cool}	σ_{cool}	k_{void}	σ_{void}	CVR	σ_{CVR}	k_{cool}	k_{void}	CVR	Δk_{cool}	Δk_{void}	ΔCVR
MWd/THE	-	-	-	-	mk	mk	-	-	mk	mk	mk	mk
LC-06b PuO_2+ThO_2 Fuel												
4.6	1.3240	0.00015	1.3379	0.00016	7.8	0.12	1.3197	1.3326	7.3	-4.4	-5.3	-0.5
11938.3	1.0465	0.00016	1.0571	0.00015	9.5	0.20	1.0419	1.0510	8.3	-4.6	-6.1	-1.2
23865.1	0.9140	0.00013	0.9233	0.00014	11.0	0.23	0.9089	0.9169	9.6	-5.0	-6.3	-1.4
LC-08b PuO_2+ThO_2 Fuel												
4.6	1.3783	0.00017	1.3943	0.00016	8.3	0.12	1.3735	1.3881	7.7	-4.7	-6.1	-0.7
18591.8	1.0458	0.00015	1.0573	0.00017	10.4	0.20	1.0402	1.0506	9.5	-5.6	-6.6	-0.8
37395.3	0.9021	0.00016	0.9120	0.00014	12.0	0.26	0.8962	0.9048	10.6	-5.9	-7.2	-1.4
LC-10b $LEUO_2$+ThO_2 Fuel												
4.6	1.2362	0.00013	1.2514	0.00015	9.9	0.13	1.2408	1.2552	9.2	4.7	3.8	-0.7
12187.2	1.0432	0.00015	1.0560	0.00014	11.6	0.19	1.0471	1.0592	10.8	3.9	3.2	-0.8
24587.4	0.9475	0.00012	0.9587	0.00014	12.4	0.20	0.9510	0.9617	11.7	3.5	3.0	-0.6
LC-12b $LEUO_2$+ThO_2 Fuel												
4.6	1.3481	0.00016	1.3643	0.00013	8.8	0.11	1.3532	1.3684	8.2	5.2	4.2	-0.6
20217.4	1.0443	0.00016	1.0579	0.00015	12.4	0.20	1.0486	1.0612	11.3	4.3	3.3	-1.0
40642.9	0.8914	0.00014	0.9020	0.00015	13.2	0.26	0.8943	0.9041	12.2	2.9	2.1	-1.0
LC-14b $^{233}UO_2$+ThO_2 Fuel												
4.6	1.2122	0.00012	1.2237	0.00013	7.7	0.12	1.2137	1.2243	7.1	1.5	0.6	-0.6
9204.5	1.0378	0.00014	1.0481	0.00013	9.5	0.18	1.0389	1.0484	8.7	1.1	0.3	-0.8
18394.0	0.9901	0.00013	1.0000	0.00014	10.0	0.19	0.9911	1.0003	9.3	1.0	0.3	-0.7
LC-16b ThO_2 Fuel												
1.2	0.0098	0.00001	0.0106	0.00001	7837.9	137.30	0.0106	0.0115	7352.8	0.8	0.9	-485.0
2525.1	0.8567	0.00011	0.8651	0.0001	11.3	0.20	0.8570	0.8645	10.1	0.3	-0.6	-1.2
5054.3	0.9030	0.00011	0.9115	0.00012	10.3	0.20	0.9038	0.9117	9.6	0.8	0.3	-0.7

The code-to-code bias decreases in value with depletion for all fuels, with the exception of the pure thorium bundle, in both cooled and voided models. This result is somewhat unexpected as previous studies performed using the ENDF/B-VII library [8] demonstrated the bias between WIMS-AECL and MCNP increased with depletion for uranium-based fuels. The agreement for CVR is within 1.5 mk for all cases studied in the 35-element configuration, with the previously discussed exception of fresh, thorium based fuel.

The cooled linear element ratings as calculated for all of the 35-element lattice concepts are presented in Table 15. The agreement between MCNP and WIMS-AECL for all lattice concepts is better than what was achieved for the 37-element fuel. It is observed that the outer ring LER has better overall agreement, though generally all LER values are well-predicted with differences between 0%-2%, where the largest errors appear for the fresh pure thorium bundle.

Table 14
35-Element Lattice Concept MCNP5 and WIMS-AECL Calculated Cooled State Linear Element Ratings

Case	Burnup (MWd/THE)	MCNP5 LER (kW/m)		WIMS-AECL LER (kW/m)		% Difference	
		Ring 1	Ring 2	Ring 1	Ring 2	Ring 1	Ring 2
PuO_2+ThO_2							
LC-06b	4.6	24.6	43.2	25.0	43.0	1.3%	-0.5%
LC-06b	11938.3	30.8	39.1	31.1	38.9	0.9%	-0.5%
LC-06b	23865.1	31.4	38.7	31.6	38.6	0.8%	-0.4%
LC-08b	4.6	22.8	44.4	23.2	44.1	1.8%	-0.6%
LC-08b	18591.8	31.4	38.7	31.7	38.5	0.9%	-0.5%
LC-08b	37395.3	31.2	38.8	31.5	38.6	0.9%	-0.5%
$LEUO_2$+ThO_2							
LC-10b	4.6	29.7	39.9	30.0	39.7	1.1%	-0.5%
LC-10b	12187.2	31.7	38.5	32.0	38.3	1.0%	-0.5%
LC-10b	24587.4	32.0	38.3	32.3	38.1	0.8%	-0.5%
LC-12b	4.6	29.0	40.3	29.3	40.1	1.1%	-0.5%

Case	Burnup (MWd/THE)	MCNP5 LER (kW/m)		WIMS-AECL LER (kW/m)		% Difference	
LC-12b	20217.4	32.6	37.9	32.9	37.7	0.9%	-0.5%
LC-12b	40642.9	32.2	38.2	32.4	38.0	0.7%	-0.4%
$^{233}UO_2$+ThO_2							
LC-14b	4.6	30.1	39.6	30.4	39.4	1.0%	-0.5%
LC-14b	9204.5	31.1	38.9	31.3	38.8	0.9%	-0.5%
LC-14b	18394.0	31.0	39.0	31.3	38.8	0.9%	-0.5%
ThO_2							
LC-16b	1.2	12.0	6.3	11.8	6.5	1.9%	-2.3%
LC-16b	2525.1	7.1	9.6	7.1	9.6	-0.2%	0.1%
LC-16b	5054.3	7.1	9.6	7.1	9.6	-0.3%	0.2%

Plots of the 89-group cell-averaged flux per unit lethargy are shown in Figure 5 with the percent differences between WIMS-AECL and MCNP in Figure 6 for a sample of fresh fuel cases (one for each mixed oxide fuel combination). Once again, the pure thorium fuel has a higher overall flux magnitude required to achieve the desired bundle power. For the plutonium/thorium cases, the code-to-code group-wise percent difference is approximately 5% across all energies and increases in magnitude to -25% for the highest energy group. For the LEU/thorium case (LC-10b) and the ^{233}U-thorium case (LC-14b), the percent differences average out to approximately zero. The pure thorium bundle case, LC-16b, has a consistent percent difference of approximately -15% for lower energy groups and up to 5% for the highest energy bin (1 – 10 MeV).

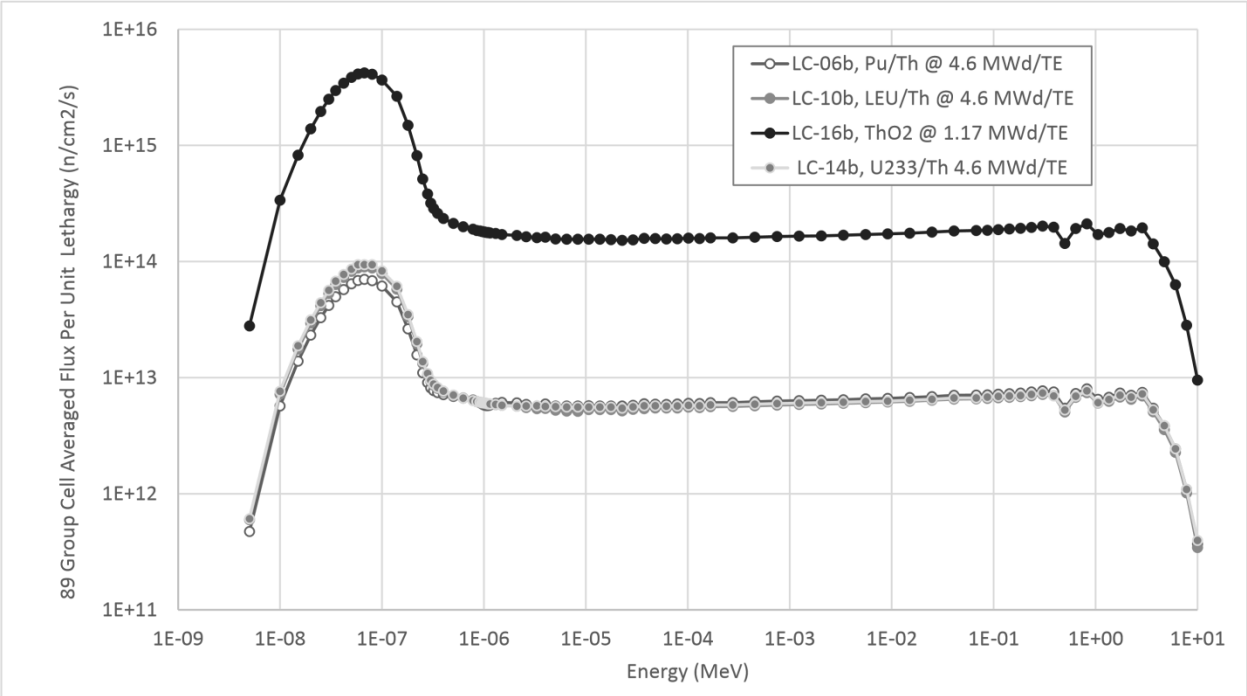

Figure 5: Cell-Averaged 89 Group Lethargy Normed MCNP Calculated Neutron Flux for 35-Element, Fresh Fuels in Cooled State.

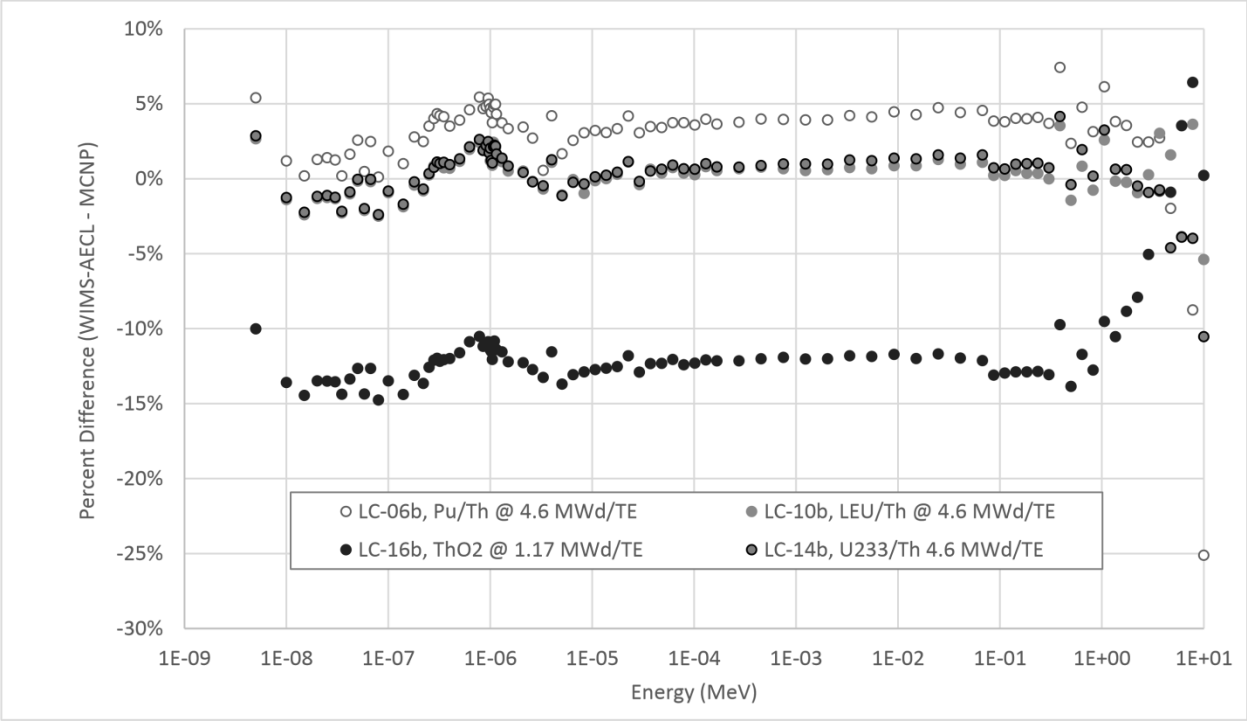

Figure 6: Cell-Averaged 89 Group Lethargy Normed Flux Percent Differences between WIMS-AECL and MCNP for 35-Element, Fresh Fuels in Cooled State.

The 89-group cell averaged fluxes and the relative error metric (as described in section 6.2) were found for each fuel configuration. Relative error values for the 35-element bundle cases are given in Table 16. Once again, the trend for the relative error is to increase with burnup (with the exception of the pure thorium bundle). There are no distinctive differences between the cooled and voided cell averaged fluxes. However, it is observed that the higher fissile content cases (LC-08b and LC-12b) result in a larger absolute error compared to the lower burnup counterparts (LC-06b and LC-10b) especially for the fresh fuel case.

Table 15
89-Group Cell Averaged Lethargy Normed Flux Absolute Error Estimates for 35-Element Fuel

Case	Burnup (MWd/THE)	Cool Error (%)	Void Error (%)
	PuO_2+ ThO_2		
LC-06b	0.46	2.4	2.9
LC-06b	11,938.30	4.0	3.7
LC-06b	23,865.13	6.7	6.6
LC-08b	0.46	3.6	4.2
LC-08b	18,591.76	4.0	3.7
LC-08b	37,395.34	6.8	6.8
	$LEUO_2$ + ThO_2		
LC-10b	0.46	1.2	1.2
LC-10b	12,187.23	4.4	4.1
LC-10b	24,587.36	6.1	6.0
LC-12b	0.46	2.2	2.6
LC-12b	20,217.35	4.1	3.8
LC-12b	40,642.86	6.9	6.8
	$^{233}UO_2$ + ThO_2		
LC-14b	0.46	1.2	1.2
LC-14b	9,204.48	3.8	3.6
LC-14b	18,394.00	4.7	4.6
	ThO_2		
LC-16b	1.17	13.2	13.4
LC-16b	2525.06	4.5	4.5
LC-16b	5054.26	4.5	4.6

7. Conclusions

WIMS-AECL and MCNP two-dimensional lattice physics models were prepared for a number of fuel compositions and geometries that could be used in a 700 MWe Pressure Tube Heavy Water Reactor. Two bundle geometries were studied, including a 37-element, four ring fuel bundle and a 35-element, two ring fuel bundle. Several fuel compositions were modelled including plutonium/thorium, low enriched uranium/thorium, pure thorium, pure uranium of varying enrichments and U-233/thorium. The ENDF/B-VII.0 nuclear data library was used, with an 89-group evaluation for the WIMS-AECL calculations and a continuous energy library in MCNP. Three stages of burnup were modelled for each fuel type: fresh, mid-burnup and exit burnup. Cooled and voided lattice cell models were prepared for each composition. Good agreement, with reasonably small discrepancies, was first obtained between WIMS-AECL and MCNP for natural uranium, 37-element fuel in the LC-01 model. This agreement was tested by comparing the results of WIMS-AECL/MCNP with available data in the literature.

The infinite eigenvalues, k-infinity cooled, k-infinity voided and CVR, evaluated for all fuel types agree well across codes. For the 37-element bundle, the average k-infinity bias for all coolant states is within +0.3 mk and the CVR bias is within +0.7 mk (with the exception of pure thorium fuel). For the 35-element fuel with a graphite central moderating element, the k-infinity average code-to-code bias for plutonium/thorium fuels is -5.0 mk, LEU/thorium containing fuels is +4.1 mk and 233-U/thorium fuels is +1.2 mk. One unexpected result is that the code-to-code differences seem to decrease in magnitude with burnup for all thorium containing fuel types with the exception of pure thorium fuels. This opposes expectations for uranium-based fuels as calculated in previous PT-HWR lattice analyses [10]. The calculated linear element ratings from both codes are within 3% for all of the cases studied. The largest code-to-code differences in LER occur in the pure, fresh thorium fuel components.

The relative error, as defined in Equation 3, captures the cumulative prediction differences in the 89-group lethargy-normed flux values that may cancel out overall in global parameters. An increase in relative error with depletion is observed in all cases with the exception of pure thorium bundles, contradicting the k-infinity bias trend observed earlier. It then follows that though the k-infinity code-to-code bias decreases with depleted fuel compositions, cancellation of errors may be occurring as there are clearly growing discrepancies between energy binned neutron fluxes predicted by WIMS-AECL and MCNP. Overall, good agreement between WIMS-AECL and MCNP was obtained for k-infinity, LER, and CVR for the fuel geometries and compositions that were studied. Further studies and improvements to the multi-group nuclear data libraries used in conjunction with WIMS-AECL may help to reduce the code-to-code differences, especially for the 89-group lethargy normed neutron fluxes and their relative errors.

8. Acknowledgements

The authors are thankful for technical help and verification from Sourena Golesorkhi. Jimmy Chow's methods for material translation were essential in completing this work. The careful reviews of Shanda Gimson, Darren Radford and Brock Sanderson are greatly appreciated.

9. References

1. OECD Nuclear Energy Agency and the International Atomic Energy Agency, “Uranium 2014: Resources, Production and Demand (The Red Book)”, (2014).
2. Y. Nakahara et al., ‘‘Nuclide Composition Benchmark Data Set for Verifying Burnup Codes on Spent Light Water Reactor Fuels,’’ Nuclear Technology, Vol. 137, No. 2, pp. 111 (2002).
3. B. P. Bromley, “Review of AECL and International Work on Sub-Critical Blankets Driven by Accelerator-Based and Fusion Neutron Sources”, Proceedings of 34th Annual Conference of the Canadian Nuclear Society, June 2013, Toronto, Ontario, Canadian Nuclear Society (2013).
4. A. Colton, B. P. Bromley, “Full Core Evaluation of Uranium Based Fuels Augmented with Small Amounts of Thorium in Pressure Tube Heavy Water Reactors”, Nuclear Technology, 2016, (in press).
5. B. Rouben, “RFSP-IST, the Industry Standard Tool Computer Program for CANDU Reactor Core Design and Analysis”, Proceedings of the 13th Pacific Basin Nuclear Conference, Oct. 2002, Shenzhen, China (2002).
6. D. V. Altiparmakov, “New Capabilities of the Lattice Code WIMS-AECL”, International Conference on the Physics of Reactors, Sep. 2008, Interlaken, Switzerland, American Nuclear Society (2008).
7. X-5 Monte Carlo Team, “MCNP-A General Monte Carlo N-Particle Transport Code, Version 5 – Vol. I: Overview and Theory,” LA-UR-03-1987, Los Alamos National Laboratory, 2005 October.
8. W. Shen, “Validation of DRAGON End-Flux Peaking and Analysis of End-Power-Peaking Factors for 37-Element, CANFLEX, and Next-Generation CANDU Fuels”, Proceedings of the 22nd Annual Conference of the Canadian Nuclear Society, June 2001, Toronto, Ontario, Canadian Nuclear Society (2001).

9. B. P. Bromley, P. Sambavalingam, and G. W. R. Edwards, `Assessment of Power and History Effects on Thorium-Based Fuels in Pressure Tube Heavy Water Reactors`, Nuclear Science and Engineering, Vol. 182, No. 3, pp. 263-286 (2016).

10. D.V. Altiparmakov, "ENDF/B-VII.0 versus ENDF/B-VI.8 in CANDU Calculations", Proc. of PHYSOR 2010, May 2010, Pittsburgh, PA, American Nuclear Society (2010).

11. A. Nuttin, P. Guillemin, T. Courau, G. Marleau, O. Meplan, et al., "Study of CANDU thorium-based fuel cycles by deterministic and Monte Carlo methods", PHYSOR-2006 Topical Meeting on Advances in Nuclear Analysis and Simulation, Sep. 2006, Vancouver B.C., American Nuclear Society/Canadian Nuclear Society (2006).

12. A. Nuttin, P. Guillemin, A. Bidaud, N. Capellan, et al., "Comparative analysis of high conversion achievable in thorium-fueled slightly modified CANDU and PWR reactors", Annals of Nuclear Energy, Vol. 40, pp. 171-189 (2011).

13. G. Roh, H. Choi, "Benchmark Calculations for Standard and DUPIC CANDU Fuel Lattices Compared with the MCNP-4B Code", Nuclear Technology, Vol. 132, pp. 128-151 (2000).